

PREPARED FOR SUBMISSION TO JHEP

Prospect of measuring the top quark mass through energy correlators

Meng Xiao, Yulei Ye, and Xinyu Zhu

School of Physics, Zhejiang University, Hangzhou, Zhejiang 310058, China

E-mail: mxiao@zju.edu.cn, ylye@zju.edu.cn, xy_zhu@zju.edu.cn

ABSTRACT: Reaching a high precision of the top quark mass is an important task of the Large Hadron Collider. We perform a feasibility study of measuring the top quark mass through the three-point energy correlator. The expected sensitivity of the top quark mass in the boosted regime is presented. We further introduce its application to the low top p_T regime and demonstrate that both the W boson and the top quark masses could be extracted from this single observable. Compared to traditional observables, the energy correlator shows robustness to uncertainties that usually dominate experimental measurements and provides a promising way to improve experimental precision.

Contents

1	Introduction	1
2	E3C and its application to top quark	2
3	Top mass sensitivity in the boosted region	2
4	E3C in the resolved regime	5
5	Conclusions	8

1 Introduction

The top quark is the heaviest elementary particle in the Standard Model. The precision of its mass, together with that of the Higgs boson, plays a central role in determining the stability of the electroweak vacuum [1–4]. While the precise measurement of the top quark mass has been one of the most important campaigns at the Large Hadron Collider (LHC), the yielded uncertainty is the largest among those of the heavy elementary particles [5].

Various strategies have been developed to precisely measure the top quark mass m_t [6–19], among which the most precise one comes from the direct measurements [10], where the top quark is treated as a free particle and Monte-Carlo (MC) based simulation is used to extract the m_t . The experimental signature and the corresponding measurement vary with the transverse momentum of the top quark p_T^{top} . The low p_T^{top} region, often called the resolved regime, presents a final state with three particles decayed from the top quark and well-separated from each other. Experiments usually reconstructed the invariant masses from the three objects to measure the m_t . As the p_T^{top} increases, the decayed products get Lorentz-boosted, making the hadronic decay products of the top quark non-resolvable and forming a single large jet. Typical observables for the m_t measurement in this regime are the invariant jet mass.

For both p_T^{top} regimes, the reconstructed invariant masses are subject to uncertainties in the jet p_T , such as the jet energy scale uncertainty (JES). Although the JES has been constrained experimentally by the precisely known W boson mass [10, 19], it still dominates the uncertainties in these measurements. Recently, energy correlators inside jets have been proposed to study the properties of heavy particles such as the top quark mass [20, 21] in the boosted regime. They have the advantage of being theoretically calculable and, therefore could be used to extract the pole mass of the top quark. These correlators have been measured for light flavor jets by the CMS collaboration [22], demonstrating that high-precision measurements of the observable could be reached.

In this paper, we illustrate that the energy correlator is an ideal observable to reduce the impact of JES in top mass measurements. It is powerful to improve the precision of

the m_t not only in the boosted regime but also in the resolved regime. We first present its sensitivity to the m_t in the boosted region using MC simulations, where the projected three-point energy correlator (E3C) is compared with the jet invariant mass m_{jet} , and better resilience to systematic uncertainties such as JES is observed. We then extend the method to the low p_T^{top} regions, where two peaks resulting from the W boson and the top quark could be observed simultaneously in the E3C distribution. The intriguing features of the peaks make the E3C a promising observable to improve the m_t precision in the resolved region.

2 E3C and its application to top quark

Multi-point energy correlators [23–25] are a class of observables that describe the energy-weighted angular correlations between particles. Specifically, the E3C focuses on the correlation among three particles. The theoretical definition of E3C is [26, 27]

$$\text{E3C} = \frac{d\sigma}{dx_L} = \sum_{i,j,k}^n \int d\sigma \frac{E_i E_j E_k}{E^3} \delta(x_L - \max(\Delta R_{ij}, \Delta R_{ik}, \Delta R_{jk})). \quad (2.1)$$

At hadron colliders, they are proposed for jet substructure studies. In its application to boosted top jets [20], the particle indices i, j, k run overall all the n particles in a top jet, and E is the summed energy of all the particles, equivalent to the jet energy. The largest $\Delta R_{ij} = \sqrt{\Delta\eta^2 + \Delta\phi^2}$ of the triangle formed by i, j, k particles is denoted by x_L . Since the top quark decays to three particles, E3C is a natural probe for the top decay. The distribution of E3C is a function of x_L with energy weight $E_i E_j E_k / E^3$. Experimental resolution of angles is much better than the energies, therefore compared to invariant mass type observables, E3C could be measured with higher precision. In addition, the weight makes the observable robust to uncertainties that systematically change the energy of the jet constituents, since the changes largely cancel in the ratio.

3 Top mass sensitivity in the boosted region

We start by examining the sensitivity of the E3C observable to the m_t in the boosted top region. MC simulation of the $t\bar{t}$ semi-leptonic process is used. According to experimental measurements [28], this process yields the highest sensitivity. The events are generated with MADGRAPH5_aMC@NLO [29, 30] at leading-order (LO) of QCD and interfaced to PYTHIA8 [31] for parton shower and hadronization. Multiple samples are generated with different top quark masses, ranging from 168 GeV to 174 GeV. The mass of the W boson is set to 80.4 GeV. To select the hadronically decayed top quark, anti- k_T algorithm [32] is performed by FastJet [33, 34] with parameter $R = 1.2$. An event is required to have at least two jets with $p_T^{\text{top}} > 400$ GeV and $|\eta| < 2.4$ and a lepton with $p_T > 60$ GeV and $|\eta| < 2.4$. The leading jet is required to be further away from the lepton compared to the sub-leading jet, and it is used to evaluate the sensitivity to the m_t .

Here we compare the performances of E3C to m_{jet} . CMS has used m_{jet} to measure the m_t with a relative uncertainty of 1.45% [11] with 36 fb^{-1} data and the uncertainty was

further reduced to 0.50% [19] after constraining JES uncertainty using the W mass with 138 fb^{-1} data. We have the choice to extract the m_t either from the reconstructed shapes at the detector level or from the unfolded shapes at the generator level. The advantage of the latter, as proposed in Ref [11], is that once theoretical calculation is available, it could be used to extract the pole mass instead of the MC mass. For this reason, here we use the generator distribution to derive the sensitivity. To have a realistic estimation of selection efficiency and statistical loss due to the unfolding procedure, we downscale the number of events so that the statistical uncertainty of m_t derived from m_{jet} is the same as the CMS result in Ref. [11]. For the comparison between the two variables, we assume the unfolding impact is similar and the same downscale factor is applied to both distributions.

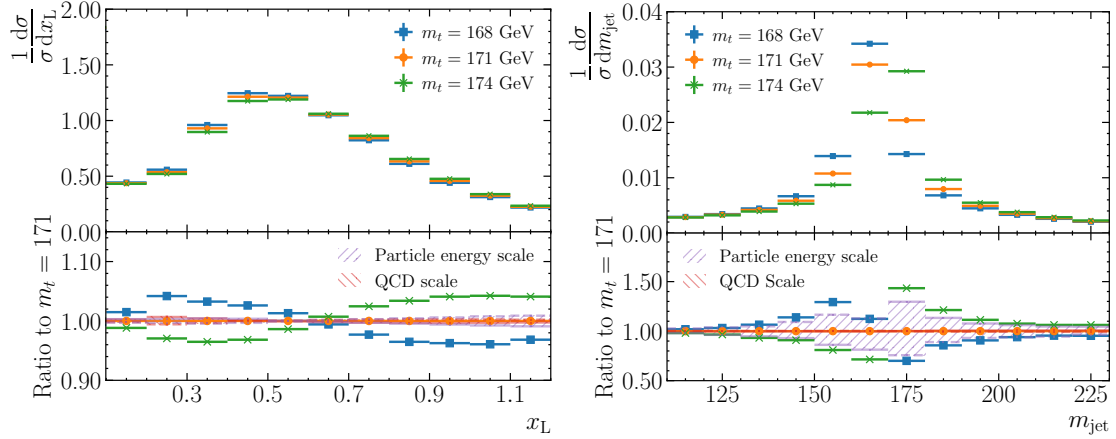


Figure 1. The distribution of E3C (left) and m_{jet} (right) of boosted top jets with different m_t values and their ratio to $m_t = 171 \text{ GeV}$. The leading systematic uncertainties are shown in hatched bands in the ratio panel. Here the photon, charged, and neutral particle energy scales are combined into the total particle energy scale.

Figure 1 shows the E3C and m_{jet} distribution built from the boosted jet. All the hadrons inside the jet are used for the calculation. A peak is observed for both observables, which originated from the top quark decay, and is sensitive to the m_t , as shown by the distributions of various m_t values. For the m_{jet} , this is rather straightforward to understand. As for the E3C, it could be explained by $x_L \propto m_t/p_T^{\text{top}}$ [20] in large p_T^{top} limit. Since p_T^{top} remains relatively constant as m_t changes, the peak position is directly proportional to the m_t . Compared to E3C, the nominal shape of m_{jet} is more sensitive to the m_t . The variation caused by a 3 GeV change in m_t is about 40% compared to 5% in the E3C. However, the same variation in m_{jet} could be caused by the jet p_T scale, as shown by the shaded distribution in figure 1. This is the reason why JES uncertainty plays an important role in such measurements [11]. On the other hand, the figure shows that E3C is much less affected by this uncertainty.

To evaluate the impact of various systematic uncertainties, we consider the sources that potentially dominate the two measurements from Ref. [11] and [22]. This includes the energy scale uncertainties of the particles within the jet, which is 1% for the charged particles, 3% for the photons and 5% for the neutral particles [22]. Each source affects

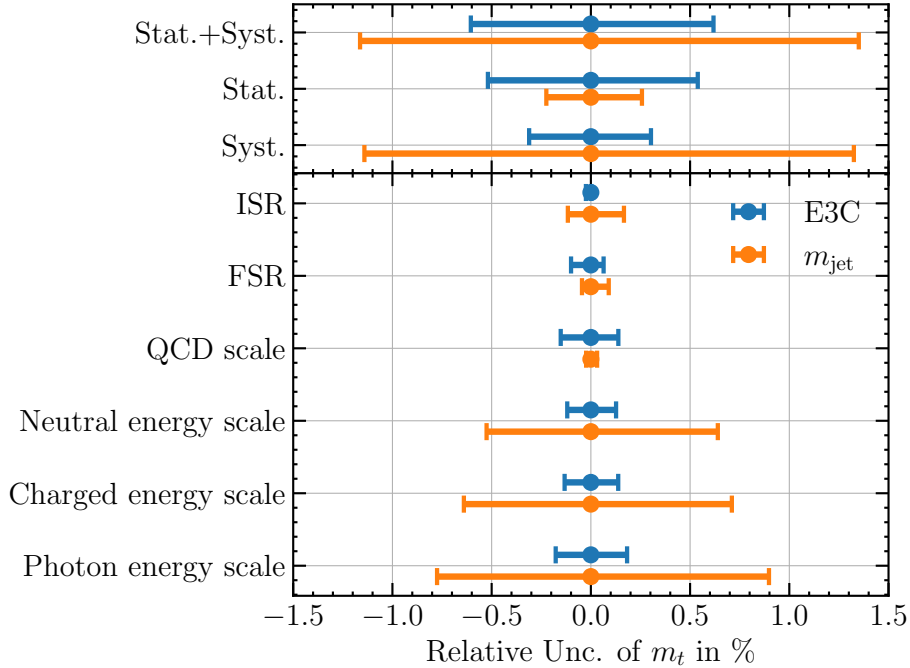


Figure 2. The expected uncertainties of m_t (in % of $m_t = 171$ GeV) using E3C and m_{jet} distributions, at $\mathcal{L} = 36 \text{ fb}^{-1}$. The statistical uncertainties and a breakdown of the systematic uncertainties are shown.

the particles of a particular type and, consequently the overall jet p_T . The combined particle energy scale effect is analogous to the JES uncertainty, which changes the jet p_T by approximately 1-2% for the jets considered here. The initial-state (ISR) and final-state radiation (FSR) uncertainties are considered by varying the renormalization scale μ in parton shower by 1/2 and 2. The QCD scale uncertainties that take into account the missing higher-order calculation in hard scattering processes are obtained from varying the renormalization and factorization scales independently by a factor of 0.5 and 2.

We calculate the χ^2 values as a function of the m_t under the impact of the above uncertainties for m_{jet} and E3C respectively. We take the shape of $m_t = 171$ GeV as the nominal, and a deviation of $\Delta\chi^2 = 1$ is used to extract the uncertainties. An integrated luminosity of 36 fb^{-1} is used. The estimated uncertainties from this analysis are presented in figure 2. The m_{jet} result is dominated by systematic uncertainties of the particle energy scales inside the jet, while the E3C based result is mainly limited by the statistical uncertainty. At the luminosity of 36 fb^{-1} , the E3C already yields a better overall sensitivity of 0.6% compared to 1.2% from m_{jet} . It is expected that the E3C based result would gain more from increased statistics. At the luminosity of 300 fb^{-1} , the statistical uncertainty for E3C will decrease to 0.2%, comparable to the systematic uncertainty.

4 E3C in the resolved regime

The most precise measurement of the m_t was derived in the low p_T^{top} region [10], benefiting from the large cross section. The measurement was systematic dominated and the JES was one of the major sources. The above studies in the boost regime have demonstrated that the E3C observable is much less affected by this uncertainty. The overall m_t precision would benefit more if the method could be extended to the low p_T^{top} region. Here the hadronically decayed top quark is no longer contained in a single jet, but rather becomes three well separated jets. Therefore we modify the E3C definition and treat the three jets as the constituents of the top quark, and the E in Eq. 2.1, which was the energy of the top quark jet, now becomes the sum of the energy of the three jets. Given that the four-momentum of a quark is well represented by the corresponding jet, this definition is even less affected by non-perturbative effects. As a start, we use the kinematic information of the three quarks decayed from the top quark to demonstrate the proof of principle.

We use the semi-leptonic $t\bar{t}$ process to check the feasibility. Events are simulated with MADGRAPH5_aMC@NLO at LO of QCD. We focus on the events with $p_T^{\text{top}} < 400$ GeV. The E3C is built from the three quarks that hadronically decayed from the top quark. As the p_T^{top} becomes comparable with the top quark mass, the dependence of the x_L on p_T^{top} and m_t becomes nontrivial. To differentiate the impact of the p_T^{top} and m_t , we split the events into slices of p_T^{top} .

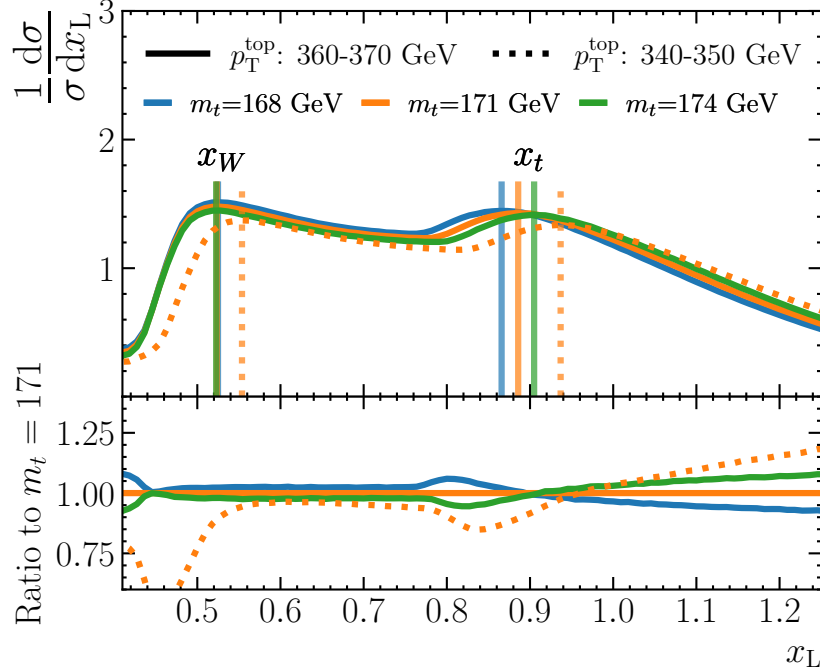


Figure 3. E3C distributions in the resolved regime in the range of $360 < p_T^{\text{top}} < 370$ GeV and $340 < p_T^{\text{top}} < 350$ GeV. The three quarks decayed from the top quark are used to build E3C. A comparison between the distributions with different m_t values is presented.

Figure 3 shows the E3C distribution in two p_T^{top} ranges: 360–370 GeV and 340–350

GeV. In each p_T^{top} range, two distinct peaks are observed, and a structure arises from distinct decays of the W boson and top quark. We simulate events with different m_t values while keeping the m_W fixed to 80.4 GeV, as shown in figure 3. The right peak shifts with the m_t while the left peak stays unchanged. This feature makes the E3C a nice observable to calibrate the m_t through m_W . In earlier experimental measurements, this was achieved by constructing several observables from different inputs [10]. However, the dominant systematic uncertainties in extracting m_t and m_W may not fully overlap and are well constrained in multiple observables. While in the case of E3C, consistent inputs are used to construct a single observable, resulting in a better constraint on the uncertainties.

Similar to the approach in the boosted regime, the shape of the E3C can be used to measure m_t in the resolved regime. The overall E3C distribution depends on p_T^{top} as shown in figure 3, therefore a joint measurement of E3C across multiple p_T^{top} regions could improve the sensitivity. However, this also makes the measurement potentially prone to the JES: a genuine $p_T^{\text{top}} = 345$ GeV event, corresponding to the dashed curve in figure 3, might be reconstructed as $p_T^{\text{top}} = 365$ GeV due to higher JES. If the distribution exhibited a single peak, similar to the often-used reconstructed m_t in experimental measurements, this curve could be interpreted as either a higher m_t or a higher JES, causing a large systematic uncertainty on the m_t . However, the W peak on the left helps to disentangle the two effects: both peaks move with JES, and only the top peak shifts with m_t variation, as shown in the ratio panel of figure 3. The two peak structure of E3C helps to reduce the impact of JES uncertainty significantly and provide a new method for experimental measurements.

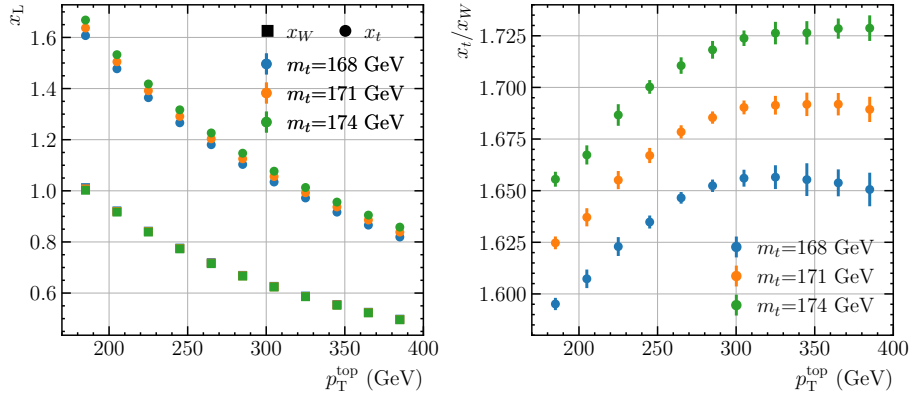


Figure 4. The peak position of x_W and x_t (left) and x_t/x_W (right) in the E3C distributions as a function of average p_T^{top} . The values are fitted from distributions under different m_t assumptions.

The observation that both peaks in the E3C distribution shift together with p_T^{top} raises the question of whether the ratio between them is less sensitive to p_T^{top} . This could be explored to further reduce the uncertainty. To quantify that, we perform a fit to identify the x_L value corresponding to the two peaks, which we denote as x_W and x_t respectively. We use an exponentially modified Gaussian function in LMFIT package [35] to fit the E3C distribution near the peaks. The fit range of x_L is determined by requiring the $\chi^2/\text{n. d.f.} < 2$. To take into account the impact of the fit range, we vary the nominal range

by 10% and take the difference between the determined peaks from the fits as a systematic uncertainty. The results are shown in figure 4. The left figure shows the extracted x_t and x_W as a function of the average p_T^{top} in each region. Both x_t and x_W decreases with increasing p_T^{top} . Under different m_t assumptions, the x_W overlaps while the x_t shows a sensitivity to the m_t value. The right figure shows the ratio of x_t/x_W as a function of p_T^{top} . The ratio has a rather strong dependency on p_T^{top} in the relatively low p_T region, while in the range above 300 GeV, it becomes flatter. Experimental measurements could use the x_t/x_W ratio in this region to reduce the sensitivity to any uncertainties that cause migrations in the reconstructed p_T^{top} .

So far, we have focused on introducing the idea of using E3C and its feature to measure the top quark mass in the resolved regime in the ideal case. Complications are expected when applying it to experimental measurements, including correctly picking jets originated from the top quark and possible degradation of E3C shape arising from jet reconstruction. For a realistic assessment of the effects, we use PYTHIA8 and Delphes [36] to simulate parton shower, hadronization and detector effects, where CMS settings are used. Jets are reconstructed by anti- k_T method with distance parameter of 0.4. For a jet with 100 GeV p_T , the energy resolution is 10%. Events are selected requiring one lepton with $p_T > 60$ GeV and four jets with $p_T > 30$ GeV, among which two should be b-tagged. All the objects are required to have $|\eta| < 2.4$. The hadronic-decayed top quark is reconstructed from the two light jets and a b-tagged jet. Between the two b-tagged jets, the one that gives a m_t^{reco} closer to 171 GeV is picked. The selection is rather crude and about 55% of the events are correctly reconstructed from the top decay quarks.

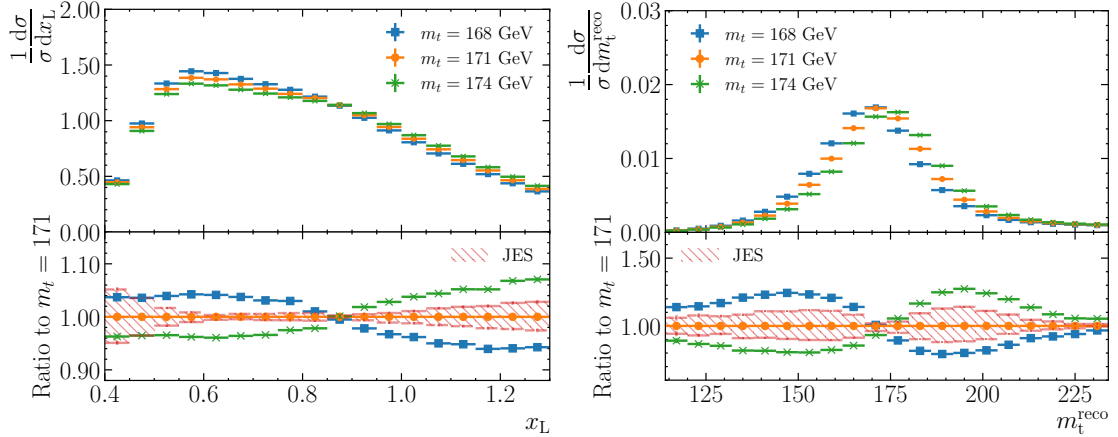


Figure 5. The normalized distribution of E3C (left) and m_t^{reco} (right) reconstructed from three jets in the resolved region in the range of $360 < p_T^{\text{top, reco}} < 370$ GeV. Different m_t values and their ratio to $m_t = 171$ GeV are shown. The JES uncertainty is shown in hatched bands in the ratio panel.

The E3C distribution built from the above selection is shown in figure 5. The reconstructed p_T^{top} is required to be within 360–370 GeV to compare with the ideal distribution in figure 3. It is clear that the two-peaks structure is smeared, however the shape dependency on m_t remains. To evaluate the impact of JES, we take its uncertainty values

from CMS [37], which varies from 2–1% for jets with p_T of 30 – 100 GeV, and 0.8% for $p_T > 100$ GeV. This causes event migrations between categories and a shape distortion. Figure 5 shows the E3C shape variation due to the JES, which is mild and different from that caused by m_t . While for the m_t^{reco} the JES and m_t effects are more similar.

We use the reconstructed E3C distribution to check its sensitivity to m_t under the JES impact, to be compared with m_t^{reco} . Events with reconstructed p_T^{top} in the range of 200–400 GeV are selected and categorized in slices of p_T^{top} , each covering a range of 40 GeV. The E3C distributions in the five categories are shown in figure 6. Two peaks are visible in all the categories and shift with $p_T^{\text{top, reco}}$. In principle finer bins could be adopted so that the peaks are sharper and help better constrain the JES. For simplicity here we use coarse binning. We calculate χ^2 as a function of m_t with JES as a nuisance parameter, which causes 2–7% event migration in the considered categories and shape changes. The expected uncertainty of m_t is shown in figure 6. Similar to the conclusion in the boosted region, E3C is less sensitive to the JES uncertainty compared to the m_t^{reco} . At the luminosity of 137 fb^{-1} , E3C already yields a better overall sensitivity. With such settings, a 0.1% sensitivity is expected for E3C at 300 fb^{-1} . On top of this, improvements are expected to further increase the sensitivity, such as exploring lower $p_T^{\text{top, reco}}$ region, finer binning in categories and better top candidate selections.

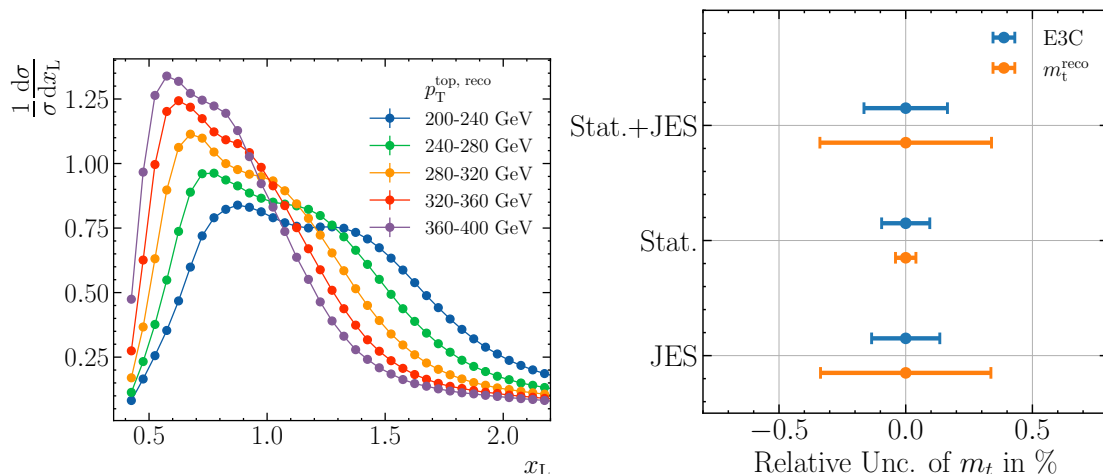


Figure 6. Left: the distribution of E3C reconstructed in five different $p_T^{\text{top, reco}}$ regions. Right: the expected uncertainties of m_t (in % of $m_t = 171 \text{ GeV}$) using reconstructed E3C and m_t^{reco} distributions in the resolved region, at $\mathcal{L} = 137 \text{ fb}^{-1}$. The statistical uncertainties and JES systematic uncertainties are shown.

5 Conclusions

In summary, we explored the potential of using E3C to determine the top quark mass in both resolved and boosted regimes. In the boosted regime, we showed that E3C provides a better mass sensitivity compared to the traditional jet mass observable in terms of systematic uncertainties, and is expected to benefit more from the increased statistics at the

LHC. In the resolved regime, the presence of two distinct peaks in the E3C distribution, corresponding to the top quark and the W boson, helps to calibrate the top quark mass and constrain jet energy scale uncertainties greatly. These results demonstrate that E3C could be a promising observable for achieving high-precision measurement of the top quark mass.

Acknowledgments

We thank Huaxing Zhu for the useful discussions. The work is supported by National Natural Science Foundation of China (NSFC) under the Grant No. 12322504 and the center for high energy physics in Peking University.

References

- [1] S. Alekhin, A. Djouadi and S. Moch, *The top quark and Higgs boson masses and the stability of the electroweak vacuum*, *Phys. Lett. B* **716** (2012) 214 [[1207.0980](#)].
- [2] G. Degrandi, S. Di Vita, J. Elias-Miro, J.R. Espinosa, G.F. Giudice, G. Isidori et al., *Higgs mass and vacuum stability in the Standard Model at NNLO*, *JHEP* **08** (2012) 098 [[1205.6497](#)].
- [3] D. Buttazzo, G. Degrandi, P.P. Giardino, G.F. Giudice, F. Sala, A. Salvio et al., *Investigating the near-criticality of the Higgs boson*, *JHEP* **12** (2013) 089 [[1307.3536](#)].
- [4] A. Andreassen, W. Frost and M.D. Schwartz, *Scale Invariant Instantons and the Complete Lifetime of the Standard Model*, *Phys. Rev. D* **97** (2018) 056006 [[1707.08124](#)].
- [5] PARTICLE DATA GROUP collaboration, *Review of Particle Physics*, *PTEP* **2022** (2022) 083C01.
- [6] CMS collaboration, *Review of top quark mass measurements in CMS*, [2403.01313](#).
- [7] ATLAS collaboration, *Measurement of the top quark mass in the $t\bar{t} \rightarrow \text{lepton} + \text{jets}$ channel from $\sqrt{s} = 8$ TeV ATLAS data and combination with previous results*, *Eur. Phys. J. C* **79** (2019) 290 [[1810.01772](#)].
- [8] CMS collaboration, *Measurement of the top quark mass using proton-proton data at $\sqrt{s} = 7$ and 8 TeV*, *Phys. Rev. D* **93** (2016) 072004 [[1509.04044](#)].
- [9] CMS collaboration, *Measurement of the top quark mass in the all-jets final state at $\sqrt{s} = 13$ TeV and combination with the lepton+jets channel*, *Eur. Phys. J. C* **79** (2019) 313 [[1812.10534](#)].
- [10] CMS collaboration, *Measurement of the top quark mass using a profile likelihood approach with the lepton + jets final states in proton-proton collisions at $\sqrt{s} = 13$ TeV*, *Eur. Phys. J. C* **83** (2023) 963 [[2302.01967](#)].
- [11] CMS collaboration, *Measurement of the Jet Mass Distribution and Top Quark Mass in Hadronic Decays of Boosted Top Quarks in pp Collisions at $\sqrt{s} = 13$ TeV*, *Phys. Rev. Lett.* **124** (2020) 202001 [[1911.03800](#)].
- [12] CMS collaboration, *Measurement of the top quark mass using events with a single reconstructed top quark in pp collisions at $\sqrt{s} = 13$ TeV*, *JHEP* **12** (2021) 161 [[2108.10407](#)].

- [13] CMS collaboration, *Measurement of the top quark pole mass using $t\bar{t}$ +jet events in the dilepton final state in proton-proton collisions at $\sqrt{s} = 13$ TeV*, *JHEP* **07** (2023) 077 [[2207.02270](#)].
- [14] ATLAS collaboration, *Top-quark mass measurement in the all-hadronic $t\bar{t}$ decay channel at $\sqrt{s} = 8$ TeV with the ATLAS detector*, *JHEP* **09** (2017) 118 [[1702.07546](#)].
- [15] CMS collaboration, *Measurement of the top quark mass using charged particles in pp collisions at $\sqrt{s} = 8$ TeV*, *Phys. Rev. D* **93** (2016) 092006 [[1603.06536](#)].
- [16] CMS collaboration, *Measurement of the mass of the top quark in decays with a J/ψ meson in pp collisions at 8 TeV*, *JHEP* **12** (2016) 123 [[1608.03560](#)].
- [17] ATLAS collaboration, *Measurement of the $t\bar{t}$ production cross-section using $e\mu$ events with b-tagged jets in pp collisions at $\sqrt{s} = 7$ and 8 TeV with the ATLAS detector*, *Eur. Phys. J. C* **74** (2014) 3109 [[1406.5375](#)].
- [18] ATLAS collaboration, *Measurement of the top-quark mass using a leptonic invariant mass in pp collisions at $\sqrt{s} = 13$ TeV with the ATLAS detector*, *JHEP* **06** (2023) 019 [[2209.00583](#)].
- [19] CMS collaboration, *Measurement of the differential $t\bar{t}$ production cross section as a function of the jet mass and extraction of the top quark mass in hadronic decays of boosted top quarks*, *Eur. Phys. J. C* **83** (2023) 560 [[2211.01456](#)].
- [20] J. Holguin, I. Moul, A. Pathak and M. Procura, *New paradigm for precision top physics: Weighing the top with energy correlators*, *Phys. Rev. D* **107** (2023) 114002 [[2201.08393](#)].
- [21] J. Holguin, I. Moul, A. Pathak, M. Procura, R. Schöffbeck and D. Schwarz, *Using the W as a Standard Candle to Reach the Top: Calibrating Energy Correlator Based Top Mass Measurements*, [2311.02157](#).
- [22] CMS collaboration, *Measurement of energy correlators inside jets and determination of the strong coupling $\alpha_S(m_Z)$* , [2402.13864](#).
- [23] C.L. Basham, L.S. Brown, S.D. Ellis and S.T. Love, *Energy Correlations in electron - Positron Annihilation: Testing QCD*, *Phys. Rev. Lett.* **41** (1978) 1585.
- [24] L.J. Dixon, I. Moul and H.X. Zhu, *Collinear limit of the energy-energy correlator*, *Phys. Rev. D* **100** (2019) 014009 [[1905.01310](#)].
- [25] K. Lee, B. Meçaj and I. Moul, *Conformal Colliders Meet the LHC*, [2205.03414](#).
- [26] H. Chen, I. Moul, X. Zhang and H.X. Zhu, *Rethinking jets with energy correlators: Tracks, resummation, and analytic continuation*, *Phys. Rev. D* **102** (2020) 054012 [[2004.11381](#)].
- [27] W. Chen, J. Gao, Y. Li, Z. Xu, X. Zhang and H.X. Zhu, *NNLL resummation for projected three-point energy correlator*, *JHEP* **05** (2024) 043 [[2307.07510](#)].
- [28] CMS, ATLAS collaboration, *Combination of measurements of the top quark mass from data collected by the ATLAS and CMS experiments at $\sqrt{s} = 7$ and 8 TeV*, [2402.08713](#).
- [29] J. Alwall, R. Frederix, S. Frixione, V. Hirschi, F. Maltoni, O. Mattelaer et al., *The automated computation of tree-level and next-to-leading order differential cross sections, and their matching to parton shower simulations*, *JHEP* **07** (2014) 079 [[1405.0301](#)].
- [30] R. Frederix, S. Frixione, V. Hirschi, D. Pagani, H.S. Shao and M. Zaro, *The automation of next-to-leading order electroweak calculations*, *JHEP* **07** (2018) 185 [[1804.10017](#)].
- [31] C. Bierlich et al., *A comprehensive guide to the physics and usage of PYTHIA 8.3*, *SciPost Phys. Codeb.* **2022** (2022) 8 [[2203.11601](#)].

- [32] M. Cacciari, G.P. Salam and G. Soyez, *The anti- k_t jet clustering algorithm*, *JHEP* **04** (2008) 063 [[0802.1189](#)].
- [33] M. Cacciari and G.P. Salam, *Dispelling the N^3 myth for the k_t jet-finder*, *Phys. Lett. B* **641** (2006) 57 [[hep-ph/0512210](#)].
- [34] M. Cacciari, G.P. Salam and G. Soyez, *FastJet User Manual*, *Eur. Phys. J. C* **72** (2012) 1896 [[1111.6097](#)].
- [35] M. Newville, T. Stensitzki, D.B. Allen and A. Ingargiola, *LMFIT: Non-Linear Least-Square Minimization and Curve-Fitting for Python*, Oct., 2015. [10.5281/zenodo.11813](#).
- [36] J. de Favereau, C. Delaere, P. Demin, A. Giammanco, V. Lemaître, A. Mertens et al., *Delphes 3: a modular framework for fast simulation of a generic collider experiment*, *Journal of High Energy Physics* **2014** (2014) .
- [37] CMS collaboration, *Jet energy scale and resolution performance with 13 TeV data collected by CMS in 2016-2018*, .